Journal of The Electrochemical Society, **163** (10) A2368-A2370 (2016)
0013-4651/2016/163(10)/A2368/3/$33.00 © The Electrochemical Society

Communication—Investigation of Anatase-TiO_2 as an Efficient Electrode Material for Magnesium-Ion Batteries

Minghao Zhang,[a] Alex C. MacRae,[a,b] Haodong Liu,[a,*] and Ying Shirley Meng[a,,z]**

[a]*Department of NanoEngineering, University of California San Diego, La Jolla, California 92093, USA*
[b]*Department of Chemistry and Biochemistry, University of California San Diego, La Jolla, California 92093, USA*

Magnesium-ion batteries (MIBs) have twofold volumetric energy density than that of lithium without the dendritic deposition morphology associated with Li, which makes MIBs attractive options. We investigate the feasibility of using anatase-phase TiO_2 as an electrode material for MIBs. Electrochemical, microscopic, and spectroscopic analyses are performed in order to probe Mg-ion insertion as well as determine the limitation of TiO_2 as a viable electrode material.

Manuscript submitted May 4, 2016; revised manuscript received July 22, 2016. Published August 31, 2016.

The commercial use of a magnesium metal is advantageous over a comparable lithium metal, as the volumetric capacity is nearly double and the deposition morphology is described as non-dendritic.[1] As such, considerable attention has been drawn to the development of MIBs over the last decades.[2,3] So far, studies of Mg rechargeable batteries are limited to a few choices of electrode materials such as vanadium oxide, Chevrel phases, molybdenum sulfide, manganese oxide, and transition metal silicates.[4–6] Although discharge capacity around 200 mAh g^{-1} has been achieved, kinetic sluggish characteristic of Mg^{2+} ion diffusion process limits the ability of inserting magnesium into these electrodes. Magnesium/sulfur batteries have been also proposed by Muldoon.[1] However, further work is needed to prevent the sulfur and polysulfides in the electrolyte from dissolving as well as the discharge capacity from decreasing from the second cycle.

Anatase TiO_2, a typical lithium intercalation electrode, is considered to be a magnesium battery cathode candidate.[7] A prototype system for magnesium/anatase TiO_2 has been reported by Sheha et al.[8] The discharge capacity is found insufficient for various applications. Wang and co-workers greatly improved magnesium insertion ability of anatase TiO_2 by employing $LiBH_4$ in $Mg(BH_4)_2$/tetraglyme electrolyte.[9] This electrolyte has large concentration of lithium salt. In order to prevent the lithium insertion interference, we decide to investigate the feasibility of TiO_2 as an electrode for MIBs in All Phenyl Complex (APC) electrolyte.[3] This electrolyte contains pure magnesium salt in THF solution and has electrochemical windows wider than 3 V. This widely acknowledged electrolyte in MIBs is thus the best candidate to examine the magnesium insertion into anatase TiO_2. Both spectroscopic and microscopic techniques have been applied to confirm the limitation of magnesium insertion into anatase TiO_2 through both electrochemical and chemical process.

Experimental

Commercially available TiO_2 (Sigma Aldrich, <20 nm particle size) was used without any additional treatment. Magnesium counter electrode was purchased from Alfa-Aesar and the surface was mechanically cleaned in an inert gas environment before it was used. The APC electrolyte preparation was described in the previous work and electrochemical test was explained in the supplementary information.[3]

Powder diffraction spectra of all samples were taken by using synchrotron XRD at the Advanced Photon Source (APS) on beamline 11-ID-C. Following a careful transfer step to avoid any exposure to oxygen, the TiO_2 electrodes were examined using scanning electron microscopy (SEM) (Phillips XL30) with the equipped energy dispersive X-ray detector (EDX). UV−vis spectra were carried out in an absorption mode on a Lambda 1050 UV−Vis spectrometer.

Results and Discussion

Electrolyte stability is a key factor in exploring the electrochemical performance of a magnesium battery system. As shown in Figure S1, APC electrolyte used in this work shows highly reversible Mg deposition with low overpotential. TiO_2 electrode is coupled with APC electrolyte to study Mg^{2+} insertion/extraction behaviors. Cyclic voltammogram of anatase TiO_2/Mg battery between 0.02 V and 2.35 V at a low scan rate of 0.1 mV s^{-1} is displayed in Figure 1a. The cathodic peaks (magnesium insertion) at around 0.8 V, 0.25 V, and the anodic peak (magnesium extraction) at around 1.7 V are observed. They are consistent with charge–discharge curve shown in Figure 1b. During the first discharge, TiO_2 exhibits a discharge capacity of ∼80 mAh g^{-1} at a current density of 5 mA g^{-1}. The material experiences a large polarization where the charge plateau increases to 1.5 V. The corresponding irreversible capacity at the first cycle is 20 mAh g^{-1}, which might have derived from the poor conductivity of the electrode. Figures 1c and 1d also illustrate discharge/charge profiles and coulombic efficiency with respect to cycle number at the same current density over 50 cycles. The capacity of the electrode remains at a quite considerable value (∼40 mAh g^{-1}) after 50 cycles. The decrease of capacity can be attributed to the side reactions between trace water absorbed onto the TiO_2 surface and electrolyte as well as corrosive reactions between electrolyte and stainless steel current collectors.[5]

In order to investigate the phase transitions, ex-situ XRD patterns were collected at different states of charge-discharge in Figure S2. The pristine electrode demonstrates a typical tetragonal anatase phase with space group I41/amd. No explicit changes are found at all different states, showing the retention of the tetragonal anatase phase. Figure 2 further shows the detailed crystal structure evolution during the first cycle based on high resolution synchrotron X-ray diffraction. Despite their similar crystal structures, Table I quantitatively shows the refined lattice parameters (a and c) for the electrode during the initial charge and discharge process. The reliability factors from the Rietveld refinements are less than 8%, which implies that the results are trustworthy to explain the crystal structure. The lattice parameters of pristine TiO_2 electrode are $a = 3.789$ Å and $c = 9.512$ Å, which are in good agreement with previous XRD study. As a comparison, the lattice parameters of fully discharged electrode are $a = 3.792$ Å and $c = 9.503$ Å. This observation confirms the slight increase of a lattice parameter and decrease of c lattice parameter. During Mg-ion insertion, a lattice parameter, which is dominated by Ti–Ti distance, increases slightly as expected from the reduced Ti ions. The shrinkage of c lattice parameter of the fully discharged electrode is due to less electrostatic repulsion between adjacent oxygen layers. Both a and c lattice parameters of the fully charged state change back to the original numbers of the pristine state. The tetragonal phase remains, signifying the good reversibility of TiO_2 electrode. It is notable that the relatively small changes of the lattice parameter result from only Mg:Ti ratio of ∼0.1:1 inserted into TiO_2 structure at the fully discharged state by the electrochemical method.

*Electrochemical Society Student Member.
**Electrochemical Society Member.
[z]E-mail: shmeng@ucsd.edu

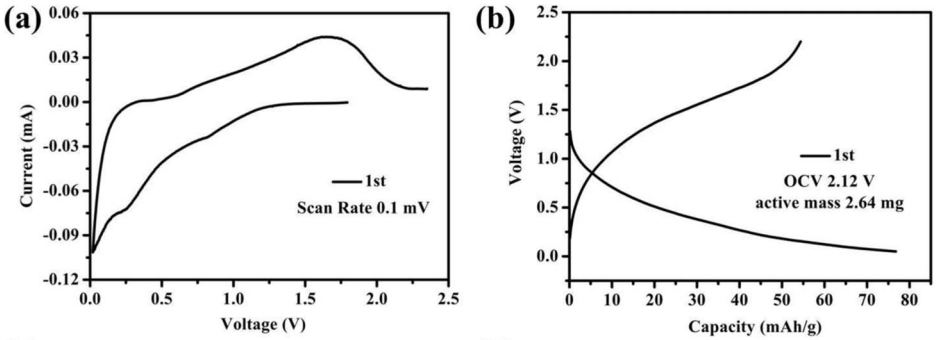

Figure 1. (a), (b) Cyclic voltammograms and first dicharge/charge curve of anatase TiO_2/Mg battery; (c), (d) discharge/charge profiles and coulombic efficiency with respect to cycle number at a current density of 5 mA g^{-1}.

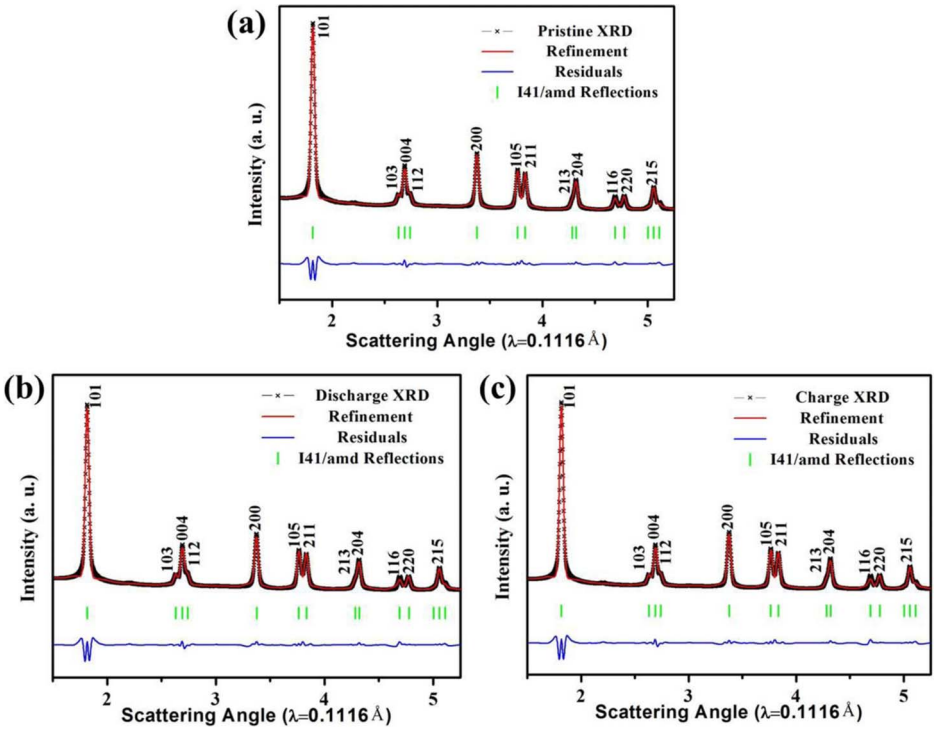

Figure 2. (a)-(c) Ex-situ synchrotron XRD patterns for the TiO_2 electrode at pristine, fully discharged and charged states, respectively.

In order to quantify Mg insertion into anatase TiO_2 structure, the electrodes were examined using EDX mapping. It is found that following discharge of the cell to 0.05 V, a magnesium signal is observed in the EDX mapping (Figure 3a). Quantitation of this result leads to a Mg:Ti ratio of ~0.1:1, which is also signified from the initial discharge capacity. To determine the ability of Mg to reversibly shuttle between the working electrode and counter electrode, magnesiated TiO_2 electrode was charged to 2.2 V and removed for SEM/EDX analysis. No obvious magnesium signal is seen in the EDX mapping (Figure 3b), indicating that magnesium ions can reversibly diffuse between the magnesium metal counter electrode and titanium dioxide working electrode.

As discussed above, a Mg:Ti ratio of ~0.1:1 can be inserted into anatase TiO_2 through electrochemical method. Chemical magnesiation was conducted using a method shown in scheme 1 to investigate the limitation of Mg insertion into anatase TiO_2. A vivid color

Table I. Rietveld refinement method fitted parameters of TiO_2 electrode.

Material	$a = b$ (Å)	c (Å)	R_{wp} (%)	R_B (%)
Pristine	3.7896(3)	9.5124(7)	6.74	3.99
Discharge	3.7927(3)	9.5039(7)	6.58	4.30
Charge	3.7908(3)	9.5086(7)	7.32	5.40

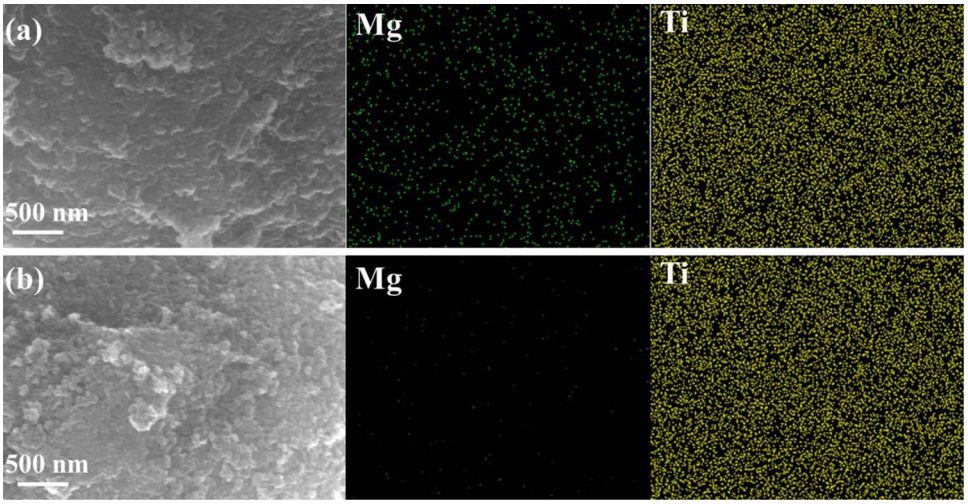

Figure 3. (a), (b) SEM/EDX mapping for the TiO_2 electrode at fully discharged and charged states, respectively.

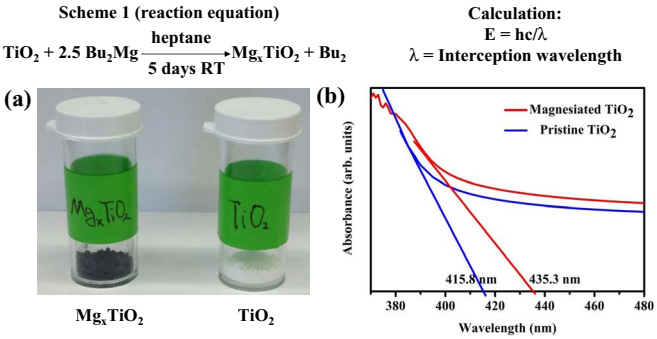

Figure 4. (a) Chemical magnesiation process and samples obtained; (b) UV−vis spectra for the pristine and magnesiated samples.

change is observed (Figure 4a), with the white TiO_2 powder suspension solution turning into dark blue color. This phenomenon has been previously described for chemical lithiation of anatase TiO_2 using the analogous *n*-butyl lithium.[10] Elemental analysis using EDX was performed in the same way onto this proprietary material. As shown in Figure S3, an apparent magnesium signal is visible in the elemental mapping, with a quantitation value nearly identical to that of the electrochemically magnesiated TiO_2. This is noteworthy because the starting stoichiometric ratio of Mg:Ti for chemical magnesiation is 1:4, not 1:10. As a result, a limited magnesiation capacity is reached for both electrochemical and chemical ion insertion.

Insertion of an electrochemically active ion into a host structure reduces one of the metal ions in the host structure. As a result, the energy difference between the valence and conduction bands of the host metal ion changes upon intercalation. This phenomenon is observed in the lithiation of TiO_2.[11] Therefore, as another method to verify the magnesium insertion into the anatase TiO_2 host structure, UV−vis spectra were carried out for the pristine and magnesiated samples (Figure 4b). As summarized in Table II, the interception wavelength of magnesiated sample increases radically compared to that of pristine TiO_2, which confirms that magnesium insertion changes the energy difference between the valence and conduction bands of the host structure. The decrease of bandgap leads to improvement of the electronic conductivity of TiO_2 after magnesiation, which indicates a good rate capability as shown in Figure S4. The material still exhibits a discharge capacity of ∼45 mAh g^{-1} at a current density of 40 mA g^{-1}.

Table II. Interception wavelength and bandgap calculated results from UV-vis spectra.

Sample	Wavelength Edge (nm)	Band Gap (eV)
Pristine	415.8	2.99
Magnesiated	435.3	2.87

Conclusions

Both spectroscopic and microscopic techniques confirm that a Mg:Ti ratio of ∼0.1:1 can be inserted into anatase TiO_2 electrochemically or chemically without phase transformation. The different insertion ability of lithium and magnesium ions into anatase TiO_2 once more manifests the sluggish kinetics of Mg^{2+} ion diffusion process.

Acknowledgments

The authors acknowledge the support by the seed funding from Sustainable Power and Energy Center under the Frontier of Innovation Award by Vice Chancellor of Research at UC San Diego. H. L. acknowledges the China Scholarship Council under Award No. 2011631005. All the authors appreciate the assistance of Dr. Yang Ren at beamline 11-ID-C of Argonne National Laboratory.

References

1. H. S. Kim, T. S. Arthur, G. D. Allred, J. Zajicek, J. G. Newman, A. E. Rodnyansky, A. G. Oliver, W. C. Boggess, and J. Muldoon, *Nat Commun*, **2**, 427 (2011).
2. Y. NuLi, Z. Guo, H. Liu, and J. Yang, *Electrochem Commun*, **9**, 1913 (2007).
3. O. Mizrahi, N. Amir, E. Pollak, O. Chusid, V. Marks, H. Gottlieb, L. Larush, E. Zinigrad, and D. Aurbach, *J Electrochem Soc*, **155**(2), A103 (2008).
4. D. Aurbach, I. Weissman, Y. Goffer, and E. Levi, *Chem Rec*, **3**(1), 61 (2003).
5. P. Saha, M. K. Datta, O. I. Velikokhatnyi, A. Manivannan, D. Alman, and P. N. Kumta, *Prog Mater Sci*, **66**, 1 (2014).
6. Y. P. Zheng, Y. N. NuLi, Q. Chen, Y. Wang, J. Yang, and J. L. Wang, *Electrochim Acta*, **66**, 75 (2012).
7. S. Y. Huang, L. Kavan, I. Exnar, and M. J. Gratzel, *Electrochem Soc*, **142**, L142 (1995).
8. E. Sheha, *Int J Electrochem Sci*, **8**, 3653 (2013).
9. S. J. Su, Z. G. Huang, Y. Nuli, F. Tuerxun, J. Yang, and J. L. Wang, *Chem Commun*, **51**, 2641 (2015).
10. M. Wagemaker, R. Krol, A. Kentgens, A. Well, and F. M. Mulder, *J Am Chem Soc*, **123**, 11454 (2001).
11. A. Stashans, S. Lunell, and R. Bergstrom, *Phys Rev B*, **53**, 159 (1996).